



# Repair of tendons treated with peracetic acid–ethanol and gamma irradiation by EDC combined with NHS: a morphological, biochemical and biomechanical study in vitro

Rong-xing Ma · Rui-feng Li · Xiao-qiang Deng · Rui-qi Qiao · Ji-kai Li · Kun-xiu Song · Shao-lin Ji · Yong-cheng Hu

Received: 23 November 2022 / Accepted: 4 February 2023 / Published online: 16 February 2023  
© The Author(s), under exclusive licence to Springer Nature B.V. 2023

**Abstract** The purpose of this study was to investigate whether 1-ethyl-3-(3-dimethylaminopropyl) carbodiimide (EDC) combined with n-hydroxysuccinimide (NHS) can repair tendon damage caused by peracetic acid–ethanol and gamma irradiation sterilization. The semitendinosus tendons of 15 New Zealand white rabbits were selected as experimental materials, and the tendons were sterilized in a solution containing 1% (v/w) peracetic acid and 24% (v/w) ethanol. After 15 kGy gamma irradiation

sterilization, the tendons were randomly divided into three groups ( $n=10$ ). The tendons were repaired with EDCs of 0, 2.5 and 5 mM combined with 5 mM NHS for 6 h, the tendons were temporarily stored at  $-80\pm^{\circ}\text{C}$ . The arrangement and spatial structure of collagen fibers were observed by light microscopy and scanning electron microscopy, the collagen type and collagen crimp period were observed under a polarizing microscope, and the collagen fibril diameter and its distribution were measured by transmission electron microscopy, from which the collagen fibril index and mass average diameter were calculated. The resistance of collagen to enzymolysis was detected by the free hydroxyproline test, and tensile fracture and cyclic loading tests of each group of tendons were carried out, from which the elastic modulus, maximum stress, maximum strain, strain energy density and cyclic creep strain were calculated. The obtained results showed that the gap between loose collagen fibers in the 0 mM control group was wider, the parallel arrangement of tendons in the 2.5 and 5 mM groups was more uniform and regular and the fiber space decreased, the crimp period in the 5 mM group was lower than that in the 0 mM group ( $P<0.05$ ), and the concentration of hydroxyproline in the 5 mM group ( $711.64\pm 77.95\ \mu\text{g/g}$ ) was better than that in the control group ( $1150.57\pm 158.75\ \mu\text{g/g}$ ). The elastic modulus of the 5 mM group ( $424.73\pm 150.96\ \text{MPa}$ ) was better than that of the 0 mM group ( $179.09\pm 37.14\ \text{MPa}$ ). Our results show that EDC combined with NHS can repair damaged

---

Rong-xing Ma, Rui-feng Li and Xiao-qiang Deng have contributed equally as co-first authors.

---

**Supplementary Information** The online version contains supplementary material available at <https://doi.org/10.1007/s10561-023-10080-6>.

---

R. Ma · Y. Hu (✉)  
Department of Bone and Soft Tissue Oncology, Tianjin Hospital, 406 Jiefang Southern Road, Tianjin 300211, China  
e-mail: huydoctor@163.com

R. Ma · R. Li · X. Deng · R. Qiao · J. Li  
Graduate School, Tianjin Medical University, Tianjin, China

K. Song  
Department of Hand and Microsurgery, Binzhou Medical University Hospital, Binzhou, Shandong Province, China

S. Ji  
Shandong Provincial Third Hospital, Shandong University, Jinan, Shandong Province, China

tendons after peracetic acid–ethanol and gamma radiation treatment, and 5 mM EDC has better morphological performance, anti-enzymolysis ability and biomechanical properties than 2.5 mM EDC.

**Keywords** Allografts · Tendon · Collagen cross-linking · Peracetic acid · 1-ethyl-3-(3-dimethylaminopropyl)-carbodiimide

## Introduction

Allograft tendons have been widely used in ligament reconstruction and tendon repair, but there is a risk of virus transmission during transplantation (Suarez et al. 2007; Eastlund 2006). To ensure the safety of tendon transplantation, peracetic acid–ethanol combined with low-dose 15 kGy gamma irradiation has been proven to be a common method for inactivating potentially harmful microorganisms (Zhou et al. 2014). Farago showed that if the biological load is lower than 1.5 cfu/item, 15-kGy dose can disinfect the tendon (Farago et al. 2021), and low-dose 15 kGy irradiation can effectively kill most microbial pathogens without affecting the material and structural properties of the tendon (Yang et al. 2019). However, after the tendon was treated with peracetic acid–ethanol solution (PES), the intramolecular and intermolecular cross-linking of collagen was damaged to some extent. Zhou et al. found that collagen fibers denatured after 1% PES treatment for 4 h (Zhou et al. 2014). After PES treatment of the tendon for 240 min, collagen fibers shrank, ruptured, and disorderly arranged, fiber space increased, and mechanical properties decreased (Xu et al. 2021). Therefore, how to reduce or repair this injury and improve the morphological characteristics of the tendon is a problem to be solved while sterilizing.

Chemical cross-linking is a stable solution that can promote the formation of covalent or ionic bonds between functional groups, reduce the gap between collagen fibers and increase the intermolecular force (Hu et al. 2019). Common chemical cross-linking agents include glutaraldehyde, genipin, and glucose. Glutaraldehyde is widely used to strengthen collagen biomaterials, which can significantly enhance the tensile strength of tendon bundles (Hansen et al. 2009), but it has strong cytotoxicity and even leads to tissue necrosis around the implanted area (Verissimo

et al. 2010). The cytotoxicity of genipin is only 0.01% of that of glutaraldehyde, and its biological safety in vivo has been widely demonstrated (Song et al. 2019), but genipin produces a dark blue color through a discoloration reaction during cross-linking, which will reduce its acceptance in clinical application (Wang et al. 2020). Glucose-derived cross-linking also occurs during radiation, which may protect bacteria or viruses in tissue from radiation (Seto et al. 2008); therefore, we did not use these reagents. The combination of the zero-length cross-linker 1-ethyl-3-(3-dimethylaminopropyl) carbodiimide (EDC) and *n*-hydroxysuccinimide (NHS) has been proven to be an effective collagen fiber cross-linking pathway (Kew et al. 2012; Enea et al. 2013; Shepherd et al. 2013).

EDC is a water-soluble, noncytotoxic and biocompatible coupling agent that provides a safe, effective and efficient amino bond cross-linking method (Ulubayram et al. 2002; Olde Damink et al. 1996a, b; Zeeman et al. 1999). NHS is also a nontoxic and biocompatible reagent that can enhance the stability of EDC cross-linking products (Ahn et al. 2013). To reconstruct the anterior cruciate ligament with polyethylene terephthalate, Cai et al. modified the ligament with EDC/NHS-cross-linked silk fibroin. The obtained results showed that the silk fibroin coating significantly improved the adhesion, proliferation and extracellular matrix secretion of fibroblasts, promoted new tissue regeneration, and enhanced the biocompatibility and remodeling process of artificial ligaments (Cai et al. 2019). Caruso et al. cross-linked the fibers with 10 and 25 mM EDCs. The obtained results showed that the mechanical properties of the cross-linked fiber group were significantly higher than those of the uncross-linked group (Caruso et al. 2004). To repair the annulus fibrosus of the intervertebral disc, Wang et al. prepared collagen gel with EDC and NHS as cross-linking agents, which showed that EDC/NHS could repair the annulus fibrosus defect and maintain nucleus pulposus integrity (Wang et al. 2017). Goodarzi et al. also used EDC/NHS cross-linked gelatin to prepare hydrogels and found that the hydrogel is suitable for corneal tissue engineering and is expected to be used as a substitute for artificial corneas (Goodarzi et al. 2019). For the selection of EDC concentration, 0.5 mol/L EDC used for collagen did not reduce cell viability, as confirmed by Scheffel et al. (2015). Powell et al. showed that the ultimate

tensile strength increased by more than 50% when the concentration of EDC was 10 mM, but when the concentration was higher than 10 mM, the ultimate tensile strength decreased to 70% of the average value of the control (Powell et al. 2006). Ahmad et al. treated collagen fibers with three EDC concentrations, 25 mM, 2.5 mM and 0.25 mM, and inoculated human semitendinosus tendon cells. It was found that lower cross-linking concentrations had potentially more optimized degradability and cell reactivity, cell adhesion and proliferation close to noncross-linked materials (Ahmad et al. 2015). Based on this, the EDC concentrations of 2.5 and 5 mM that we used can be considered to be noncytotoxic in biomaterials.

We studied the morphological, biochemical and biomechanical similarities and differences of tendons treated with EDC/NHS cross-linked PES and explored whether EDC/NHS can improve the destruction of tendons caused by sterilization to provide a theoretical basis for the preparation of clinical allogeneic tendons.

## Materials and methods

### Tendon acquisition and grouping

Eighteen New Zealand white rabbits aged 6 months were selected, and their body weights of 2.5~3.5 kg were in good condition (provided by the Experimental Animal Laboratory of Tianjin Orthopedic Institute, Animal Ethics No.: 2021 Medical Review 089). A 20% (w/w) Uratan solution was prepared with normal saline, which was used for animal anesthesia, and euthanasia was performed after intravenous air embolism. A total of 36 semitendinosus tendons were cut off under aseptic operation, and the para-tendon tissue on the surface was removed. After sealing, the samples were frozen at  $-80 \pm 3$  °C. According to the concentration of EDC, they were divided into three groups: the experimental group (2.5 mM group, 5 mM group) and blank control group (0 mM group).

### Tendon treatment process

The tendons sealed in aseptic sample bags were frozen at  $-80 \pm 2$  °C for 30 to 90 days. The tissue was rewarmed at room temperature and rinsed with sterile saline 3 times for 20 min each time, and the loose

connective tissue near the tendon and the muscle tissue of the muscle and tendon junction were removed. One-time pulse cleaning was performed, and the tendon blood and fat components were thoroughly removed until there was no blood or fat. The tendon was placed in a tabletop constant temperature shaker (constant temperature of 25 °C) with 95% pure ethanol for continuous degreasing for 96 h, replaced once every 12 h, and rinsed repeatedly with deionized water 3 times for 10 min each time. The PE, anhydrous ethanol and distilled water at the volume ratio of 1:24:75 were prepared into a mixed solution containing 1% (w/w) PE and 24% (v/v) anhydrous ethanol; the tendons were immersed in the mixed solution, and kept at room temperature for 120 min, irradiated with 15 kGy gamma radiation using a  $^{60}\text{Co}$  radiation source under dry ice. The inactivated tendon was placed in an aseptic centrifuge tube, PBS buffer was added at a mass volume ratio of 1:50, the tube was washed at room temperature for 1 h in a shaker, and the fluid was changed every 20 min. Repeat shock cleaning until the PBS buffer pH after cleaning is in the range of 6.5 to 7.5. The tendons and EDC (Hefei BASF Biotechnology Company, TO200-5G) were prepared at a mass ratio of 1:2, and the tendons were soaked in 50 mmol/L MES buffer for 24 h. For 0 mM group, since no cross-linking is used, we use aseptic normal saline to immerse at room temperature for 6 h to ensure dummy incubations. For the 2.5 mM group, the tendons were treated with an EDC cross-linking solution containing 50 mmol/L MES, 2.5 mmol/L EDC, and 5 mmol/L NHS (Nanjing Dulai Company 6066-82-6), and tendons were cross-linked at room temperature for 6 h with 40% ethanol (pH=5.5). For 5 mM group, the tendons were treated with an EDC cross-linking solution containing 50 mmol/L MES, 5 mmol/L EDC, and 5 mmol/L NHS, and tendons were cross-linked at room temperature for 6 h with 40% ethanol (pH=5.5). Then rinsed twice with 95% ethanol and 20~30 min/wash. Use PBS rinse twice, 12 h/wash. The HEPES buffer was rinsed 4 times, 15~20 min/wash. The tendons were prefrozen to  $-80$  °C, and then stored at  $-80 \pm 3$  °C.

### Morphological observation

#### *Light microscopy*

In each group, 3 samples were selected and longitudinally cut into 1~3 mm<sup>3</sup> sections. The specimens were

fixed in 10% formalin solution for 24 h and embedded in paraffin. Longitudinal sections with a thickness of 4  $\mu\text{m}$  were cut from the paraffin sections and collected on glass slides for staining. Then, the samples were stained with hematoxylin–eosin (HE) and Masson staining (Yeh et al. 2007).

#### *Polarizing microscopy*

The section specimens were fixed in 10% neutral formalin solution for 24–48 h, gradually dehydrated with gradient alcohol, and then dehydrated and cleared in xylene solution until the tendons were transparent. Routine paraffin sections were obtained with a thickness of approximately 5  $\mu\text{m}$ . Paraffin was removed from the sections of xylene and stained with Sirius red. Rinse with running water for 1 h and then pour into distilled water for a while. Then, the samples were soaked in Sirius red picric acid solution and dyed for 15–30 min. After dehydration and sealing, the cells were observed by polarizing microscopy.

#### *Scanning electron microscopy*

The sliced specimens were immersed in PBS, and the cell surface was rinsed with 3% glutaraldehyde precooled at 4  $^{\circ}\text{C}$  and fixed at 4  $^{\circ}\text{C}$  for 2 h or overnight. The fixed agent was washed twice with PBS every 10 min, fixed with 1% osmium acid precooled at 4  $^{\circ}\text{C}$  for 1 h, and then washed twice with PBS every 10 min. Then, the samples were dehydrated with isoamyl acetate for 30 min, dehydrated with alcohol, and then immersed in 100% acetonitrile. After vacuum drying, the samples were removed and observed under an electron microscope.

#### *Transmission electron microscopy*

The sliced specimens were fixed in 1% osmium tetroxide solution (0.1 M phosphate buffer, pH 7.4) for 2 h and then washed with phosphate buffer 3 times. The samples were continuously dehydrated in an alcohol gradient and embedded in Epon812 (SPI). The samples were transversely cut into ultrathin sections by an ultramicro cutting machine (Leica UC7) and observed under TEM (Xu et al. 2021). At least 5 parts were randomly selected to shoot the images with magnifications of X10000 and X20000, and the images of X20000 were analyzed by ImageJ/Fiji

software (Schindelin et al. 2012). Based on the classification results of Trainable Weka Segmentation, the tendon density, collagen fiber index and mass mean diameter were calculated (Suzuki et al. 2015; Jones 1991).

#### Enzymatic degradation experiment

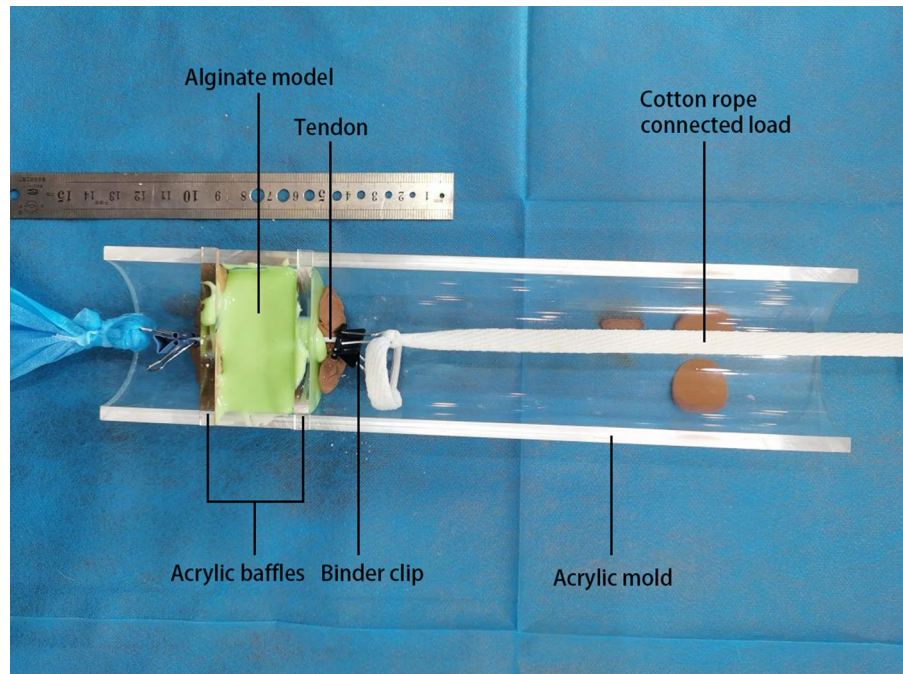
Three tendons in each group were washed with deionized water for 5 min, cut into small 5  $\text{mm}^3$  pieces, cut and dehydrated at room temperature for 24 h, and weighed. A Tris–HCl buffer solution (pH 7.8) containing 50 mM  $\text{CaCl}_2$  and 0.1%  $\alpha$ -chymotrypsin was prepared. The tendon block was placed into a 1.5 ml centrifuge tube. The 1.5 ml Tris–HCl buffer solution was added to the centrifuge tube and gently shaken in a constant temperature shaker at 37  $^{\circ}\text{C}$  for 24 h. After incubation for 24 h, the digested sample was centrifuged at a rotational speed of 14000r for 10 min, and the supernatant was fixed to 1.5 ml with distilled water. A hyp detection kit (Solarbio, Beijing, China) was used to measure the concentration of hyp in the supernatant. The standard solution of hydroxyproline and the blank solution without hydroxyproline were equally divided and detected by the kit. The OD value was recorded, the standard calibration curve was established, and the content of hydroxyproline in tissue was calculated.

#### Biomechanical tests

##### *Cross-sectional area*

The cross-sectional area of tendons in each group was measured and recorded by the alginate molding technique (Fig. 1). Vaseline was applied to lubricate the surface of the tendon; one end of the tendon was fixed, and a constant tension of 10 N was placed horizontally on the other end; sufficient alginate powder was mixed with deionized water to form a sticky tendon, and the tendon tissue was completely embedded at room temperature for solidification. The tendon embedded in alginate was extracted, and the solidified alginate was cut vertically into thin slices at intervals of 1 cm. ImageJ software was used to calculate the fissure area in each alginate section and its average value, which was the cross-sectional area of the tendon (Ge et al. 2020, 2021).

**Fig. 1** The cross-sectional area of the tendon was measured by the alginate molding technique. The lower end of the cotton rope is connected with a weight of 10 N. The cotton rope, tendon and binder clip are clamped on the same line horizontally on the table with rubber clay. The tendon is clamped by a binder clip through the central hole of the acrylic baffles, fixed and stabilized, and then viscous alginate hydrate is added



### *Cyclic loading test*

After the biomechanical fixture was cold-treated with liquid nitrogen, the two ends of the tendon were fixed on the fixture of the BOSE-ELF3230 biomechanical machine (BOSE Company, USA), the tendon was straightened, and the working distance between the two ends of the fixture was set to 1 cm. First, the load force is adjusted to 2 N for 30 s to eliminate creep. The distance between the two clamps was  $L_1$ , then the tendon was cyclically loaded at a frequency of 0.2 Hz for 50 cycles under a load force of 2–10 N, and the load-elongation curve was made according to the output results. At the same time, the length of the tendon was measured to be  $L_{10}$  after 50 cyclic loadings, and the creep value was calculated to be  $(L_{50}-L_1)/L_1$  (Yanke et al. 2013).

### *Tensile fracture test*

The tendon was given a fixed tension of 10 N for 3 min to remove creep, the load of the biomechanical machine was adjusted to 0, and then the tendon was loaded to the tendon fracture at a displacement speed of 10 mm/min. The type of tendon fracture (middle segment fracture or clamp fracture) was recorded. The stress–strain curve of each tendon was drawn by Origin2021

(OriginLab Corporation, Northampton, MA, USA), and the mechanical properties of the tendon were calculated. It includes stiffness, maximum force, maximum elongation, elastic modulus, maximum stress, maximum strain and strain energy density.

### Statistical analysis

SPSS 21.0 (SPSS Company, USA) statistical software was used for statistical analysis. The measurement data are expressed as  $\bar{X} \pm SD$ . Count data are expressed as percentages. Continuous variables that had a normal distribution and homogeneity of variance were compared by one-way ANOVA between groups, and data that did not have a normal distribution or homogeneity of variance were compared by the Kruskal–Wallis test. The LSD method was used for the post hoc test. The  $\alpha$  value of the test level is 0.05 on both sides.

## Results

### Morphological observation

The obtained results of HE staining showed that in the 0 mM group, collagen fibers were wavy and arranged

in parallel bundles, tendon cells were scattered, the fiber gap was wide, and the connection between tendon bundles was loose. In the 2.5 mM group, the tendons were arranged in parallel, the fiber space decreased and became denser, and the distribution of tendon cells was more compact and roughly parallel to the longitudinal axis of the tendon; while in the 5 mM group, the tendon was arranged in parallel, the tendon bundle space was small and uniform, and the fiber arrangement was the most compact (Fig. 2). Masson staining showed that the collagen of the tendon in the 0, 2.5 and 5 mM groups was arranged in parallel, and the staining results of each group were significantly different. The proportion of red in the 0 mM group was large, the proportion of blue in the 2.5 mM group was the second highest, and the proportion of blue in the 5 mM group was the highest.

The normal collagen was blue, and the denatured collagen was red in Masson's trichrome staining (Fig. 3). SEM showed that the tendon muscle showed a similar shape, which was composed of parallel collagen fibers with a steep waveform, and the tendon was composed of tightly packed collagen bundles wrapped in loose connective tissue. These bundles are further subdivided into smaller bundles by the sheath. When the magnification is up to 5000 $\times$ , the smooth surface of dense collagen fibers can be seen. The collagen fibers in the 0 mM group are disordered and irregular, the fibers are entangled together, the waveform is disordered, and the arrangement is loose and disorderly. In the 2.5 mM group, the collagen was arranged regularly, and the interstitial space was denser between the 0 mM group and the 5 mM group. In the 5 mM group, the collagen arrangement was the most uniform and

**Fig. 2** HE staining results of tendons treated with different concentrations of EDC. The tendon cells were scattered, and the fibers were loosely arranged in the 0 mM group (A, B 0 mM group); the fiber gap was significantly reduced, and the structure was tighter in the 2.5 mM group (C, D 2.5 mM group); the collagen gap was the narrowest in the 5 mM group (E, F 5 mM group). A, C, E ( $\times 100$ ) and B, D, F ( $\times 400$ )

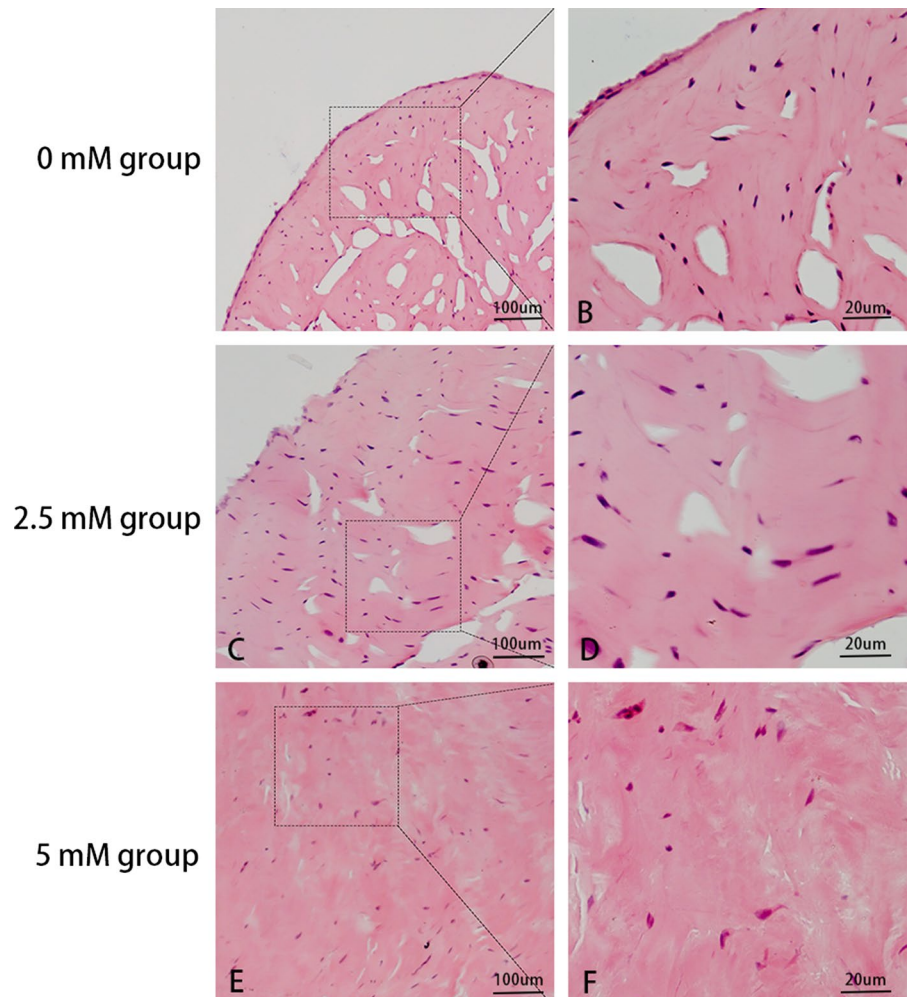
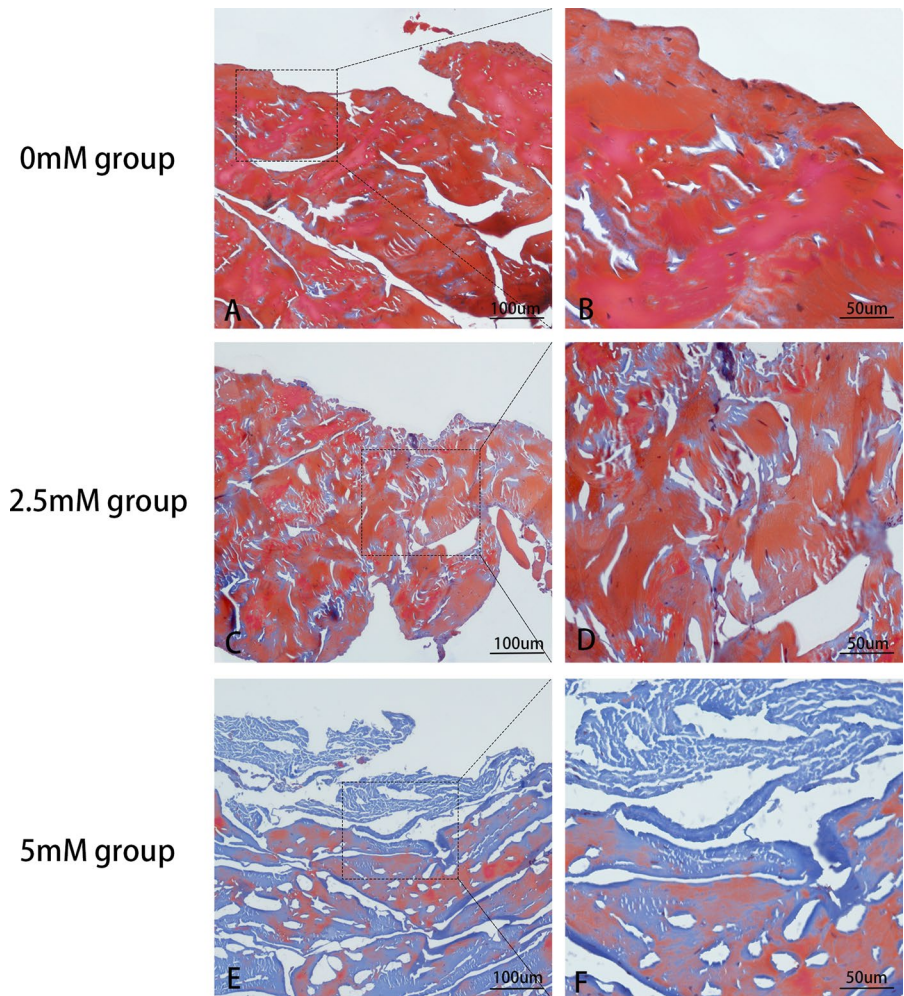


**Fig. 3** Masson staining results with different concentrations of EDC. In the 0 mM group, most of them were red, and the proportion of blue was very small (A, B 0 mM group). The proportion of the blue 2.5 mM group (C, D 2.5 mM group) was higher than that in the control group, and most of the collagen fibers returned to blue in the 5 mM group (E, F 5 mM group). A, C, E ( $\times 100$ ) and B, D, F ( $\times 400$ )



regular, the tendon fibers were cross-linked, and the space was the tightest (Fig. 4).

The structure of the collagen network can be clearly observed with polarized light; it is observed that type I collagen fibers are thick and bright yellow with a relatively large proportion, while type III collagen fibers are thin green with a relatively small proportion. The collagen structure was clearly shown in the three groups, and the fiber density was smaller and the gap was loose in the control group; the density increased in the 2.5 mM group, while it was clear that the fiber gap of the 5 mM group was the smallest and the density was the highest. The collagen crimp periods of the 0 mM group, 2.5 mM group and 5 mM group were  $71.87 \pm 6.02$ ,  $37.91 \pm 3.31$  and  $32.89 \pm 0.81$   $\mu\text{m}$ , respectively, and the difference was statistically significant ( $P < 0.01$ ); however, there was

no significant difference between the 2.5 and 5 mM groups ( $P < 0.01$ ). The crimp period increases with increasing cross-linking concentration, and denser folds can be seen in the 5 mM group (Figs. 5 and 6).

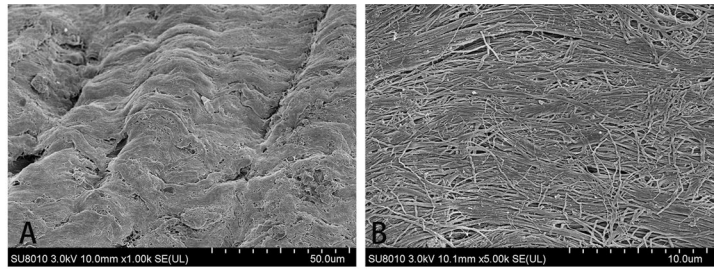
#### Fibril diameter and distribution

TEM evaluation showed that the average diameters of the 0, 2.5 and 5 mM groups were  $91.33 \pm 19.70$ ,  $136.67 \pm 3.44$  and  $157.33 \pm 10.03$  nm, respectively; the 5 mM group showed the largest average diameter, and the difference was statistically significant ( $F = 40.96$ ,  $P < 0.01$ ); the densities of 0, 2.5 and 5 mM groups were  $89.36 \pm 26.41$ ,  $67.11 \pm 5.09$  and  $57.90 \pm 7.59$   $\text{N}/\mu\text{m}^2$ , respectively, and the difference was statistically significant ( $F = 6.03$ ,  $P = 0.012$ ). The CFI values were  $62.77 \pm 1.50\%$ ,  $75.34 \pm 1.76\%$ ,

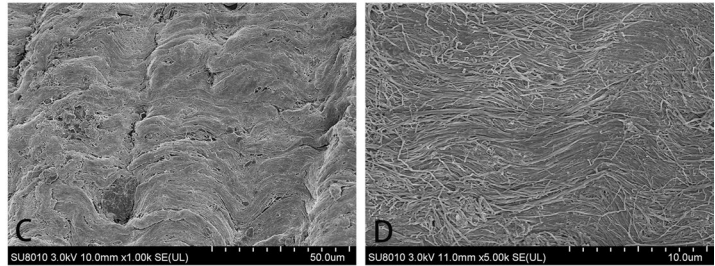
**Fig. 4** SEM results.

The collagen fibers were arranged in a disorderly and intertwined manner in the 0 mM group (A, B 0 mM group). The degree of collagen disorder decreased in the 2.5 mM group (C, D 2.5 mM group). The arrangement of collagen was the most uniform and regular, and the collagen was arranged in a wave shape in parallel in the 5 mM group (E, F 5 mM group). A, C, E ( $\times 1000$ ) and B, D, F ( $\times 5000$ )

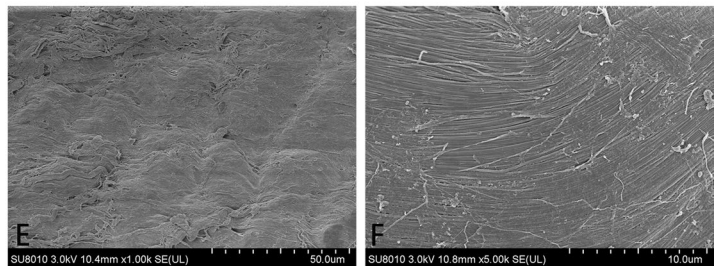
0mM group



2.5mM group



5mM group



and  $80.52 \pm 0.48\%$ , respectively, and the differences were statistically significant ( $F=268.29$ ,  $P<0.01$ ). The MAD results showed that the 0 mM group was  $223.06 \pm 5.25$  nm, and the 2.5 and 5 mM groups were  $227.35 \pm 21.85$  and  $258.86 \pm 17.58$  nm, respectively. The obtained results in the 0 mM group were the smallest, and the difference was statistically significant ( $F=8.45$ ,  $P=0.003$ ) (Fig. 7, Table 1).

The distribution of 0, 2.5 and 5 mM groups showed a double peak similar to normal distribution; the peak values of the 0 mM group were at 60 and 160 nm, and the distribution was asymptotic before and after the two peaks; in the 2.5 mM group, the peaks were at 80 and 220 nm, and the distribution on the left and right sides of the peak was asymptotic; in the 5 mM group, the peaks were at 120 and 180 nm, and there was an asymptotic change on both sides of the peak (Fig. 8).

#### Resistance to collagen degradation

The hydroxyproline concentrations of the 0, 2.5 and 5 mM groups were  $1150.57 \pm 158.75$ ,  $1061.75 \pm 160.62$  and  $711.64 \pm 77.95$   $\mu\text{g/g}$ ,

respectively. There was a significant difference among the three groups ( $F=14.153$ ,  $P<0.01$ ). The concentration of the 5 mM group was lower than that of the 2.5 and 0 mM groups ( $P<0.01$ ), but there was no significant difference between the 0 and the 2.5 mM groups by a post hoc test ( $P=0.3$ , Fig. 9).

#### Biomechanical test

Among the cross-sectional areas of tendons, the CAS values of the 0, 2.5 and 5 mM groups were  $2.03 \pm 0.29$ ,  $1.81 \pm 0.25$  and  $1.71 \pm 0.47$   $\text{mm}^2$ , respectively. The 0 mM group had the largest cross-sectional area, followed by the 2.5 and 5 mM groups, but there was no significant difference between the three groups ( $F=1.30$ ,  $P=0.30$ ) (Table 2). The cyclic loading showed that the creep strain was the smallest in the 5 mM group, at  $60.11 \pm 17.47\%$ , followed by  $165.20 \pm 65.44\%$  in the 2.5 mM group, and  $204.33 \pm 135.73\%$  in the 0 mM group. The difference between the three groups was statistically significant ( $F=4.351$ ,  $P=0.032$ ), and there was a difference



**Fig. 5** Sirius red staining results (polarized light microscopy). Type I collagen fibers were bright yellow, a small portion of type III collagen fibers were fine green, and the fiber gap was large in the 0 mM group (A, B 0 mM group). In the 2.5 mM group, the fiber crimp period increased, and the gap shrank (C, D 2.5 mM group). In the 5 mM group, the fiber order was the strongest, and denser folds could be seen (E, F 5 mM group). A, C, E ( $\times 100$ ) and B, D, F ( $\times 400$ )

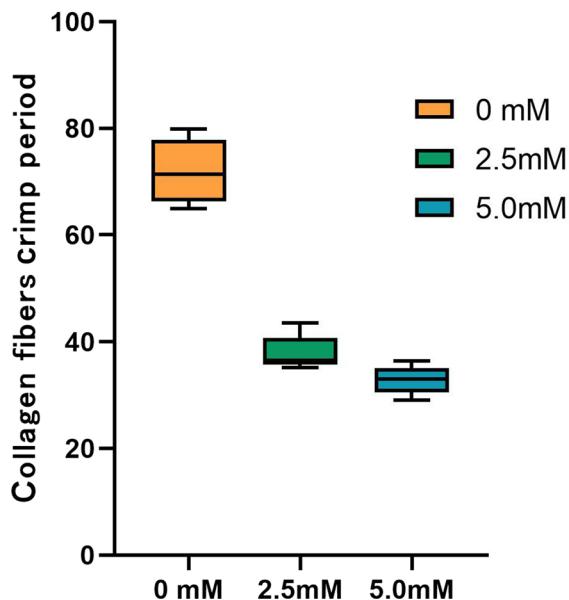
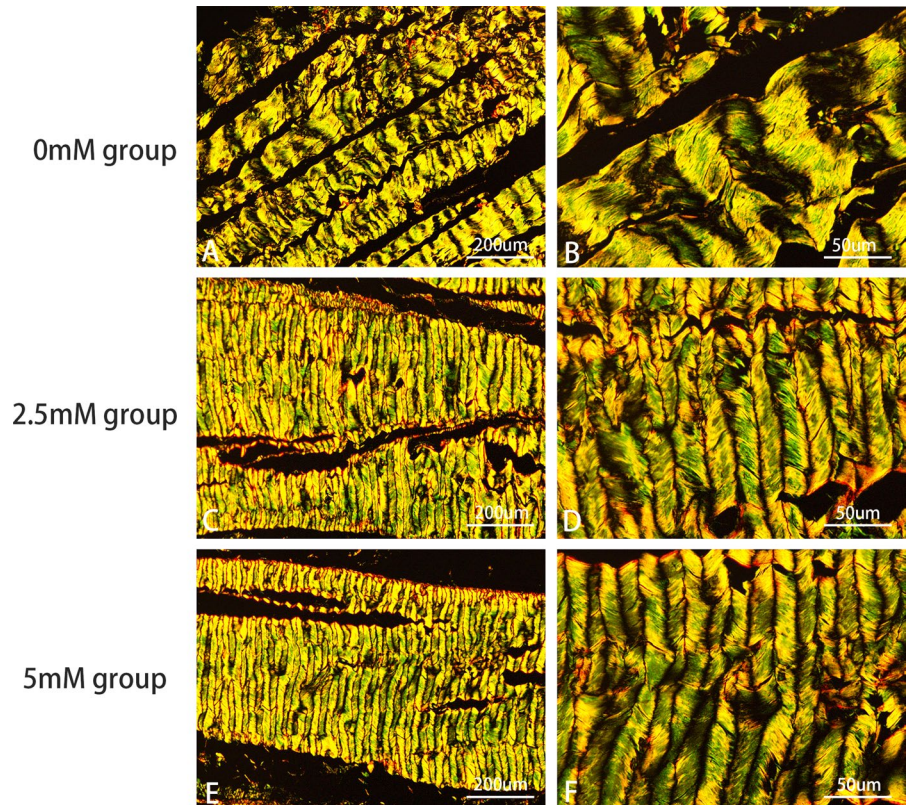


**Fig. 6** Box diagram of the collagen crimp period. The collagen crimp period in the 0 mM group, 2.5 mM group and 5 mM group was  $71.87 \pm 6.02$ ,  $37.91 \pm 3.31$  and  $32.89 \pm 0.81$   $\mu\text{m}$ , respectively, and the difference between the three groups was statistically significant ( $P < 0.01$ )

between the 0 mM group and the 5 mM group after the LSD test ( $P = 0.012$ ) (Table 2).

In tensile fracture experiments, the stiffness and elastic modulus of the 5 mM group were  $68.81 \pm 16.65$  N/mm and  $424.73 \pm 150.96$  MPa, respectively, which were significantly better than the  $36.25 \pm 7.93$  N/mm and  $179.09 \pm 37.14$  MPa in the 0 mM group ( $P = 0.002$  and  $P = 0.001$ , respectively). The stiffness and elastic modulus of the 2.5 mM group were better than those of the control group ( $P = 0.054$ ,  $P = 0.044$ ) and inferior to those of the high-concentration group. The maximum force results were  $120.338 \pm 21.912$  N for the 5 mM group,  $118.116 \pm 20.274$  N for the 2.5 mM group,  $115.40 \pm 9.124$  N for the 0 mM group, and the 5 mM group performed well, but the difference was not statistically significant ( $P = 0.894$ ). However, among the maximum stresses, the 5 mM group value ( $72.53 \pm 6.84$  MPa) was significantly higher than those of the 2.5 mM ( $63.88 \pm 11.54$  MPa) and 0 mM ( $57.79 \pm 8.30$  MPa) groups, and the difference between the three groups was statistically

**Fig. 7** The flow chart of TEM analysis by Fiji (X20000). **A** is the original picture of tendon TEM; **B** is the Fiji software machine learning to segment the fibril (red) from the background (green); **C** is the use of Threshold and Watershed Technology to completely separate the fibril; **D** is the software to count the number and area of each ellipse

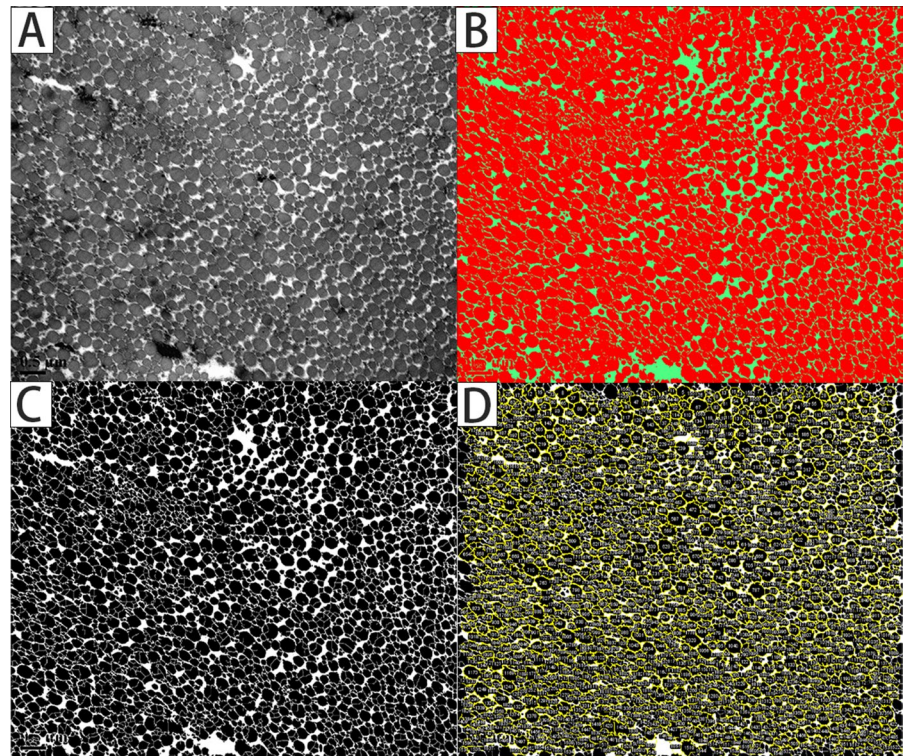


**Table 1** Statistical analysis of fibril diameter from TEM images

Groups	Mean diameter (nm)	Density (number/ $\mu\text{m}^2$ )	CFI (%)	MAD (nm)
0 mM	$91.33 \pm 19.70$	$89.36 \pm 26.41$	$62.77 \pm 1.50$	$223.06 \pm 5.25$
2.5 mM	$136.67 \pm 3.44$	$67.11 \pm 5.09$	$75.34 \pm 1.76$	$227.35 \pm 21.85$
5 mM	$157.33 \pm 10.03$	$57.90 \pm 7.59$	$80.52 \pm 0.48$	$258.86 \pm 17.58$
	$F=40.96$	$F=6.03$	$F=268.29$	$F=8.45$
	$P<0.01$	$P=0.012$	$P<0.01$	$P=0.003$
0 mM–2.5 mM	$P<0.01$	$P=0.03$	$P<0.01$	$P=0.005$
0 mM–5 mM	$P<0.01$	$P=0.004$	$P<0.01$	$P=0.002$
2.5 mM–5 mM	$P=0.014$	$P=0.338$	$P<0.01$	$P=0.658$

Indicates statistical significance the one-way analysis of variance ( $P<0.05$ ); CFI: collagen fibril index; MAD: mass average diameter

significant ( $F=3.971$ ,  $P=0.041$ ). The maximum strain for the 0 mM group was  $53.82 \pm 28.67\%$ ,  $48.67 \pm 9.44\%$  for the 2.5 mM group, and  $33.83 \pm 15.75\%$  for the 5 mM group, but there was no significant difference between the three groups ( $F=1.673$ ,  $P=0.221$ ). The strain energy densities of the 5 mM ( $31.35 \pm 8.99$ ) and 2.5 mM ( $28.79 \pm 9.29$ ) groups were higher than those of the 0 mM group ( $20.54 \pm 7.23$ ), and there was a statistically significant difference between the 5 and 0 mM groups ( $P=0.036$ ) (Fig. 10, Table 2).

## Discussion

Peracetic acid–ethanol and gamma rays have been proven to be effective in disinfecting allograft tendons. Although both methods can cause damage to the tendon, we chose a radiation dose of 15 kGy in this study, because the low dose has a slight or even negligible effect on the material and structure of the tendon (Yang et al. 2019), the injury is not clinically significant. But 1% PE can denature, wrinkle and fracture collagen fibers, increase fiber gap and reduce mechanical properties (Zhou et al. 2014; Xu

**Fig. 8** Diameter distribution of collagen fibrils. The distribution of the 0, 2.5 and 5 mM groups showed double peaks similar to normal distribution. The peaks of the 0 mM group were at 60 and 160 nm; those of the 2.5 mM group were at 80 and 220 nm, and those of the 5 mM group were at 120 nm and 180 nm

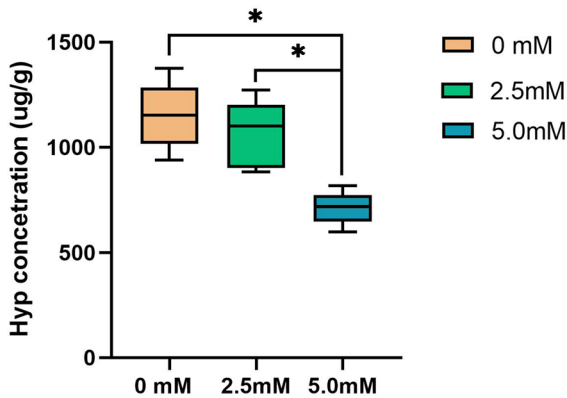
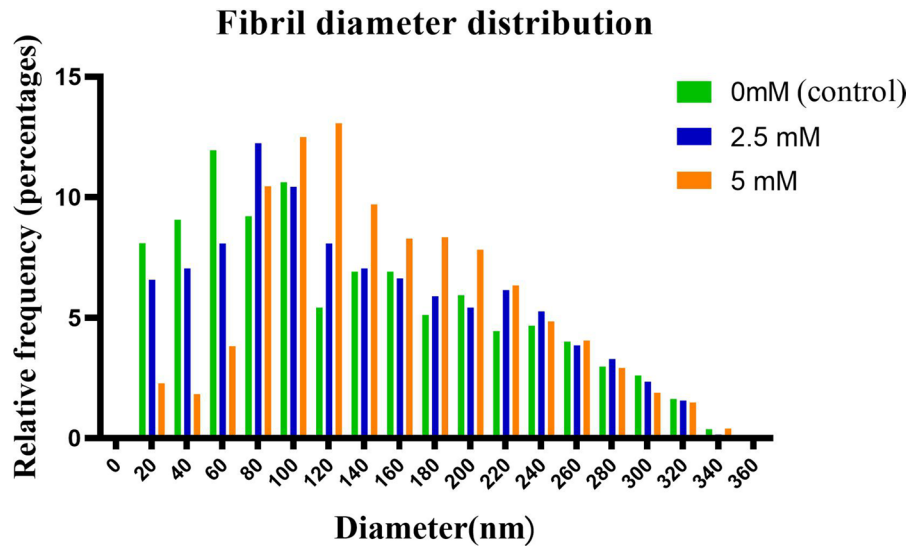


**Fig. 9** Box diagram of hydroxyproline removed per gram of tendon during digestion. (\*:  $P < 0.05$ )

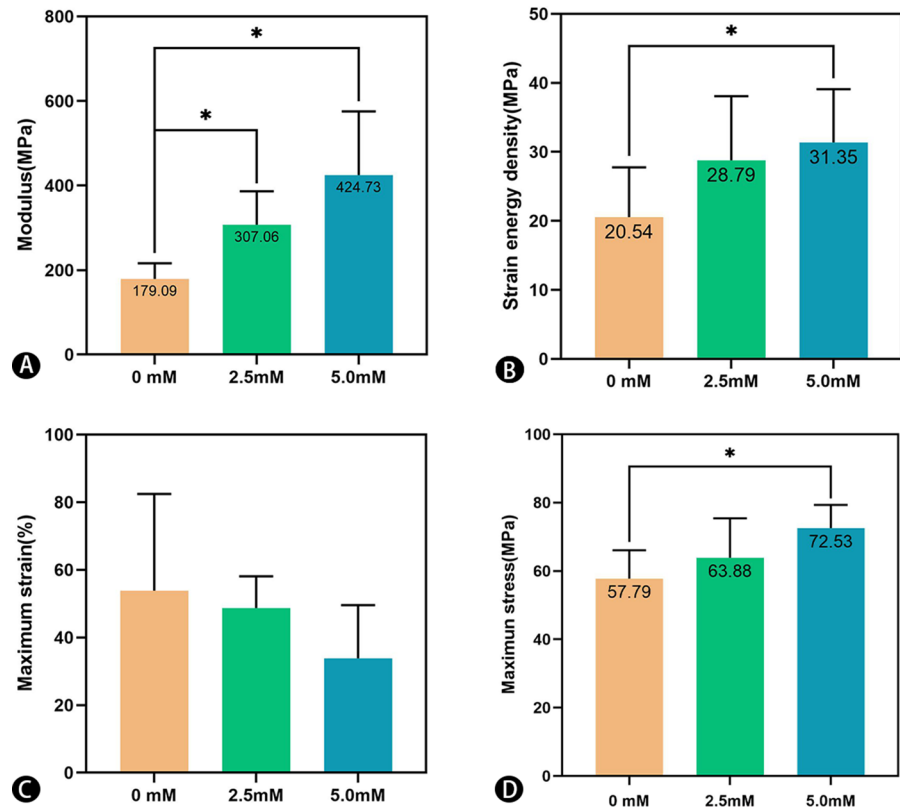
et al. 2021). Therefore, we can assume that this injury is mainly caused by PE, focusing on the analysis of its effect on tendons. The choice of EDC concentration also has a great influence on the morphology of the tendon. When the EDC concentration is high, rapid surface cross-linking will occur. The highly cross-linked fiber surface can limit the cross-linking solution from penetrating into the fiber so that the interior is completely free of cross-linking (Caruso et al. 2004). When the concentration is low, the lower degree of cross-linking of collagen cannot achieve the desired effect. To maintain the original three-dimensional structure and special function of porcine acellular dermal matrix scaffolds, Hu et al. modified the scaffold with dehydrogenation heat combined with

**Table 2** Biomechanical and material properties of different tendons

Groups	CSA (mm <sup>2</sup> )	Cyclic creep strain (%)	Stiffness (N/mm)	Max. force (N)	Max elongation (mm)	Elastic modulus (MPa)	Max stress (MPa)	Max strain (%)	Strain energy density (MPa)
0 mM	2.03 ± 0.29	204.33 ± 135.73	36.25 ± 7.93	115.40 ± 9.124	5.38 ± 2.87	179.09 ± 37.14	57.79 ± 8.30	53.82 ± 28.67	20.54 ± 7.23
2.5 mM	1.81 ± 0.25	165.20 ± 65.44	54.58 ± 18.85	118.116 ± 20.274	4.87 ± 0.94	307.06 ± 79.18	63.88 ± 11.54	48.67 ± 9.44	28.79 ± 9.29
5 mM	1.71 ± 0.47	60.11 ± 17.47	68.81 ± 16.65	120.338 ± 21.912	3.38 ± 1.57	424.73 ± 150.96	72.53 ± 6.84	33.83 ± 15.75	31.35 ± 8.99
	$F = 1.30$	$F = 4.351$	$F = 6.898$	$F = 0.113$	$F = 1.673$	$F = 8.926$	$F = 3.971$	$F = 1.673$	$F = 2.897$
	$P = 0.30$	$P = 0.032$	$P = 0.008$	$P = 0.894$	$P = 0.221$	$P = 0.003$	$P = 0.041$	$P = 0.221$	$P = 0.086$
0 mM–2.5 mM	$P = 0.303$	$P = 0.451$	$P = 0.054$	$P = 0.798$	$P = 0.657$	$P = 0.044$	$P = 0.265$	$P = 0.657$	$P = 0.099$
0 mM–5 mM	$P = 0.135$	$P = 0.012$	$P = 0.002$	$P = 0.642$	$P = 0.099$	$P = 0.001$	$P = 0.013$	$P = 0.099$	$P = 0.036$
2.5 mM–5 mM	$P = 0.616$	$P = 0.055$	$P = 0.126$	$P = 0.834$	$P = 0.211$	$P = 0.061$	$P = 0.121$	$P = 0.211$	$P = 0.592$

Indicates statistical significance using the one-way analysis of variance ( $P < 0.05$ ); CSA: cross-sectional area

**Fig. 10** Biomechanical properties in different groups. **A:** elastic modulus; **B:** strain energy density; **C:** maximum strain; **D:** maximum stress (\*:  $P < 0.05$ )



different concentrations of EDC (2.5, 7.5, 15, 25, 40 and 80 mM). The obtained results showed that when the concentration of EDC was between 2.5 mM and 7.5 mM, the cross-linking density of the EDC group significantly increased from 33.62% to 50.12% (Hu et al. 2013). To improve the mechanical properties and degradation rate of collagen scaffolds, Powell et al. used 0, 1, 5, 10, and 50 mM EDC to cross-link lyophilized collagen, and the obtained results suggested that moderate concentrations of EDC, especially 5 mM, increased the stability and strength of collagen scaffolds while providing an environment conducive to cell attachment, proliferation, and tissue growth (Powell et al. 2006). Therefore, the EDC concentrations of 2.5 and 5 mM that we used can ensure a better cross-linking effect and performance in biomaterials (Scheffel et al. 2015).

In this study, after cross-linking with EDC and NHS, the histological analysis of the tendon showed that the collagen structure changed, including smoothing some areas of collagen curl, narrowing the collagen gap, adhesion of collagen bundles to each other (which was more obvious in the 5 mM group than in

the 2.5 mM group), and the holes in a small part of the tissue were filled or reduced. This result shows that EDC forms an amide bond between collagen by activating the carboxylic acid group of glutamic acid or aspartic acid residue to react with the amine group on another chain, thus filling or narrowing the gap (Enea et al. 2013; Caruso et al. 2004). However, the uncross-linked tendons showed larger interstitial fibers, which was consistent with the obtained results of Lomas et al. who used the PE treatment (Lomas et al. 2004).

The obtained results also showed that after EDC cross-linking, the decrease and order of the collagen gap were more obvious, and the degree of decrease and orderly change in the 5 mM group were more obvious than those in the 2.5 mM group. Histological observation was also supported by the increase in collagen content in tissue degeneration. What is more interesting is that in Masson staining, the tendons treated with PES showed mostly red color, while the normal tendons should be blue (Huang et al. 2018). After cross-linking, the denatured red color was restored to blue, which was the highest in the 5 mM

group and was significantly higher than that in the 2.5 and 0 mM groups. The essence of Masson dyeing is the relationship between tissue structure density, void size and dye molecular size, which means that the tissue permeability decreases after cross-linking, and macromolecular dyes cannot pass through this to show the original blue color (Xiao et al. 2019; Li et al. 2019a, b), indicating that the 5 mM group has the lowest tissue permeability. In the experiment of Zhou et al., we also observed similar results; the tendons treated with PE stained with VG appeared yellow, while the normal collagen was red and the denatured collagen was yellow (Zhou et al. 2014).

SEM can visualize the finer structure of collagen fibers. The collagen fibers in the 0 mM group were disordered, and the gap was very large. After cross-linking, this change was very obvious, and the degree of collagen clutter in the 2.5 mM group decreased more uniformly. The collagen arrangement in the 5 mM group was the most uniform and regular, and collagen was wavy and parallel. Regarding the destruction of tendons caused by PE, Lomas et al. explained that the decomposition of PE caused oxygen bubbles in the matrix (Lomas et al. 2004). On the other hand, EDC cross-linking formed a cross-linking bond between the carboxyl group of glutamic acid and aspartic acid and the amino group of lysine, which reconnected the loose tendon bundle treated with PE. The cross-linking treatment under the polarizing microscope also showed that the gap became narrower, and the crimping period of the cross-linked tendon was shorter. The crimping cycle is a unique feature of tendon tissue, which is formed by the covalent bonding of fibrils (Edwards et al. 2017). Fibrils in turn are composed of hydroxylation of proline and lysine residues between protocollagen units, which provides stability for the collagen structure (Birch et al. 2013). Macroscopically, the morphology of the collagen curl is related to the mechanical function of tendons, and there is evidence that there is a strong specificity between the characteristics of collagen curls and the load strength of tendons. The function of the collagen curl is to act as a stress buffer, providing immediate longitudinal elongation under load. In tendons, crimp may protect the tendon structure in the event of muscle contraction and a sudden increase in joint load (Lee et al. 2019). The smaller is the crimp period of the cross-linked tendon, the greater is the corresponding tensile resistance.

Under TEM, we found that the average diameter of fibrils treated with PES was the smallest, and the average diameter of collagen fibrils after cross-linking was higher than that of the 0 mM group, and that of the 5 mM group was also higher than that of the 2.5 mM group, which is consistent with the result of Nicholls et al. who soaked tendons with PE (Nicholls et al. 1984). We know that collagen fibrils are the smallest tendon structural unit; they are mainly composed of long rod-like collagen molecules arranged at the beginning and end of a 1/4 staggered array. Collagen fibers are composed of collagen fibrils and bound by endothelin (Cui et al. 2020), which is the microstructure basis of tendons. The high tensile strength of tendons and ligaments is associated with the presence of large-diameter collagen fibrils because of the higher density of intermolecular collagen cross-linking of large-diameter collagen fibrils (Li et al. 2019a, b). There is no doubt that we use cross-linking agents to increase the cross-linking density of tendons, which will help to enhance the tensile strength of tendons. CFI is the area covered by tendon collagen fibrils, and when the diameter of the fibrils increases, the area will increase, which is consistent with the change in average diameter. In MAD, the obtained results were positively correlated with the EDC concentration, and the highest value was shown in the 5 mM group, followed by the 2.5 mM group. MAD reflects the proportion of large diameter fibrils. The higher is the value, the higher is the proportion of larger fibrils. The diameter of the fibril affects the tendon strength and elasticity. With the increase in the number of large collagen fibrils, the tensile strength increases, while the elasticity increases with the increase in small collagen fibrils (Takahashi et al. 2021). This shows that cross-linking can clearly improve the tension strength of the tendon, but the elasticity of the tendon will be weakened, which is also the reason for the macroscopic rigidity of the cross-linked tendon. Through the fibril diameter distribution map, it was found that the peak values of the 0 mM group were at 60 and 160 nm, there were double peaks at 80 and 220 nm in the 2.5 mM group, there were double peaks at 120 and 180 nm in the 5 mM group, and the peak value increased with increasing EDC concentration. The fibril is small and unimodal at birth and becomes larger and shows a bimodal distribution at maturity (Schmidt et al. 2019). After cross-linking, the bimodal distribution

of fibril size is optimized, and the larger fibril will provide higher tensile strength.

Regarding the anti-enzymolysis ability of collagen, we found that the concentration of hydroxyproline in the cross-linked tendon decreased after chymotrypsin treatment, which indicated that the resistance of collagen to enzymes was enhanced. The stability of the internal structure of the tendon depends on the intermolecular and intramolecular cross-linking components of collagen fibers. Because  $\alpha$ -chymotrypsin can only hydrolyze collagen fibers whose triple helix structure is destroyed, testing the ability of tendon to resist enzymolysis can reflect the stability of collagen and the degree of destruction from the side. The damaged tendon will release more free hydroxyproline when digested by  $\alpha$ -chymotrypsin; thus, the concentration of hydroxyproline in PE-treated tendon is higher. In addition, cross-linking makes it impossible for enzymes to fully contact collagen molecules, and enzyme decomposition can only be performed on limited-contact collagen molecules. The closure of the collagen matrix network reduces its permeability to enzymes, thus slowing down the speed of collagenase entering the matrix (Lomas et al. 2004). In addition, when the EDC concentration is too high, the highly cross-linked fiber surface can limit the penetration of the cross-linked solution into the fiber interior. Caruso et al. also confirmed that a significant surface cross-linking effect was observed when the concentration of EDC was higher than 10 mM (Caruso et al. 2004). Our results show that the enzyme resistance of 5 mM is better than that of 2.5 mM, which can at least be considered to indicate that 5 mM has no surface cross-linking, and the cross-linking properties are positively correlated in this range.

In the biomechanical test, the cross-linked tendon has better biomechanics. In the tensile fracture test, the elastic modulus of the cross-linked tendon is larger than that of the 0 mM group, the maximum stress and maximum strain are also significantly improved after cross-linking, and the strain energy density and stiffness are also improved after cross-linking. In the cyclic loading experiment, the cyclic creep strain of the tendon decreased, which indicated that the anti-creep effect of the cross-linked tendon was enhanced. At the same time, we found that the cross-sectional area of tendons decreased after cross-linking, but there was no statistical significance between the groups. This occurs due to the reduction

of the gap between tissues and the compact combination of more fibers. Macroscopically, it shows a decrease in cross-sectional area, but this microscopic change will not make a significant difference macroscopically.

However, this study also has limitations. New Zealand rabbits were selected because of the lack of access to human tendons, which still has a certain gap compared with human beings, and failed to consider the effects of confounding variables, such as donor age and sex, on the experimental results. Therefore, in future research, we will consider implanting human tendon grafts into the human body for observation and observe compatibility and adaptability with the human body.

## Conclusion

EDC combined with NHS can repair damaged tendons after peracetic acid–ethanol and gamma irradiation treatment, and the EDC concentration of 5 mM has better micromorphological characteristics, anti-enzymolysis ability and biomechanical properties than 2.5 mM. The treatment of the cross-linking method after tendon sterilization can not only inactivate the micro-organisms to ensure the safety of transplantation but also reduce the damage of sterilization to tendon collagen fibers.

**Acknowledgements** The authors are grateful the supports from Tianjin Hospital. We would also like to thank the friends who gave us help in the creation and revision of the article.

All authors listed meet the authorship criteria according to the latest guidelines of the International Committee of Medical Journal Editors, and all authors are in agreement with the manuscript.

## Declarations

**Conflict of interest** This research did not receive any specific grant from funding agencies in the public, commercial, or not-for-profit sectors.

## References

- Ahmad Z, Shepherd JH, Shepherd DV, Ghose S, Kew SJ, Cameron RE, Best SM, Brooks RA, Wardale J, Rushton N (2015) Effect of 1-ethyl-3-(3-dimethylaminopropyl) carbodiimide and N-hydroxysuccinimide concentrations on the mechanical and biological characteristics of cross-linked collagen fibres for tendon repair. *Regen Biomater* 2:77–85. <https://doi.org/10.1093/rb/rbv005>

- Ahn JJ, Kuffova L, Merrett K, Mitra D, Forrester JV, Li F, Griffith M (2013) Crosslinked collagen hydrogels as corneal implants: effects of sterically bulky vs. non-bulky carbodiimides as crosslinkers. *Acta Biomater* 9:7796–7805. <https://doi.org/10.1016/j.actbio.2013.04.014>
- Birch HL, Thorpe CT, Rumian AP (2013) Specialisation of extracellular matrix for function in tendons and ligaments. *Muscles Ligaments Tendons J* 3:12–22. <https://doi.org/10.11138/mltj/2013.3.1.012>
- Cai J, Zhang L, Chen J, Chen S (2019) Silk fibroin coating through EDC/NHS crosslink is an effective method to promote graft remodeling of a polyethylene terephthalate artificial ligament. *J Biomater Appl* 33:1407–1414. <https://doi.org/10.1177/0885328219836625>
- Caruso AB, Dunn MG (2004) Functional evaluation of collagen fiber scaffolds for ACL reconstruction: cyclic loading in proteolytic enzyme solutions. *J Biomed Mater Res A* 69:164–171. <https://doi.org/10.1002/jbm.a.20136>
- Cui J, Ning LJ, Yao X, Zhang Y, Zhang YJ, He SK, Zhang Z, Ding W, Luo JC, Qin TW (2020) Influence of the integrity of tendinous membrane and fascicle on biomechanical characteristics of tendon-derived scaffolds. *Biomed Mater* 16:015029. <https://doi.org/10.1088/1748-605X/abc203>
- Eastlund T (2006) Bacterial infection transmitted by human tissue allograft transplantation. *Cell Tissue Bank* 7:147–166. <https://doi.org/10.1007/s10561-006-0003-z>
- Edwards JH, Herbert A, Jones GL, Manfield IW, Fisher J,ingham E (2017) The effects of irradiation on the biological and biomechanical properties of an acellular porcine superflexor tendon graft for cruciate ligament repair. *J Biomed Mater Res B Appl Biomater* 105:2477–2486. <https://doi.org/10.1002/jbm.b.33786>
- Enea D, Gwynne J, Kew S, Arumugam M, Shepherd J, Brooks R, Ghose S, Best S, Cameron R, Rushton N (2013) Collagen fibre implant for tendon and ligament biological augmentation. In vivo study in an ovine model. *Knee Surg Sports Traumatol Arthrosc* 21:1783–1793. <https://doi.org/10.1007/s00167-012-2102-7>
- Farago D, Kozma B, Kiss RM (2021) Different sterilization and disinfection methods used for human tendons - a systematic review using mechanical properties to evaluate tendon allografts. *BMC Musculoskelet Disord* 22:404. <https://doi.org/10.1186/s12891-021-04296-4>
- Ge XJ, Zhang L, Xiang G, Hu YC, Lun DX (2020) Cross-sectional area measurement techniques of soft tissue: a literature review. *Orthop Surg* 12:1547–1566. <https://doi.org/10.1111/os.12757>
- Ge X, Ding J, Wang M, Li Q, Hu Y, Lun D, Zhang L, Wang L, Wang W, Liu B (2021) A novel alginate localization molding technique for cross-sectional area measurement of human tendon to access biomechanical properties. *Cell Tissue Bank* 22:11–24. <https://doi.org/10.1007/s10561-020-09858-9>
- Goodarzi H, Jadidi K, Pourmotabed S, Sharifi E, Aghamolaei H (2019) Preparation and in vitro characterization of cross-linked collagen-gelatin hydrogel using EDC/NHS for corneal tissue engineering applications. *Int J Biol Macromol* 126:620–632. <https://doi.org/10.1016/j.ijbio.2018.12.125>
- Hansen P, Hassenkam T, Svensson RB, Aagaard P, Trappe T, Haraldsson BT, Kjaer M, Magnusson P (2009) Glutaraldehyde cross-linking of tendon–mechanical effects at the level of the tendon fascicle and fibril. *Connect Tissue Res* 50:211–222. <https://doi.org/10.1080/03008200802610040>
- Hu Y, Liu L, Dan W, Dan N, Gu Z, Yu X (2013) Synergistic effect of carbodiimide and dehydrothermal crosslinking on acellular dermal matrix. *Int J Biol Macromol* 55:221–230. <https://doi.org/10.1016/j.ijbiomac.2013.01.009>
- Hu W, Wang Z, Xiao Y, Zhang S, Wang J (2019) Advances in crosslinking strategies of biomedical hydrogels. *Biomater Sci* 7:843–855. <https://doi.org/10.1039/c8bm01246f>
- Huang YZ, Wang JJ, Huang YC, Wu CG, Zhang Y, Zhang CL, Bai L, Xie HQ, Li ZY, Deng L (2018) Organic composite-mediated surface coating of human acellular bone matrix with strontium. *Mater Sci Eng C Mater Biol Appl* 84:12–20. <https://doi.org/10.1016/j.msec.2017.11.002>
- Jones PN (1991) On collagen fibril diameter distributions. *Connect Tissue Res* 26:11–21. <https://doi.org/10.3109/03008209109152160>
- Kew SJ, Gwynne JH, Enea D, Brookes R, Rushton N, Best SM, Cameron RE (2012) Synthetic collagen fascicles for the regeneration of tendon tissue. *Acta Biomater* 8:3723–3731. <https://doi.org/10.1016/j.actbio.2012.06.018>
- Lee AH, Elliott DM (2019) Comparative multi-scale hierarchical structure of the tail, plantaris, and Achilles tendons in the rat. *J Anat* 234:252–262. <https://doi.org/10.1111/joa.12913>
- Li N, Zhou L, Xie W, Zeng D, Cai D, Wang H, Zhou C, Wang J, Li L (2019) Alkaline phosphatase enzyme-induced biomineralization of chitosan scaffolds with enhanced osteogenesis for bone tissue engineering. *Chem Eng J* 371:618–630. <https://doi.org/10.1016/j.cej.2019.04.017>
- Li Y, Wu B, Qiu Z, Liang D, Liu H, Zhong M, Xu J, Chen K, Feng W, Li H et al (2019b) A correlation study between the Mohawk expression level and the collagen fiber diameter of hamstring tendon graft after anterior cruciate ligament reconstruction. *Zhongguo Xiu Fu Chong Jian Wai Ke Za Zhi* 33:1095–1101. <https://doi.org/10.7507/1002-1892.201902040>
- Lomas RJ, Jennings LM, Fisher J, Kearney JN (2004) Effects of a peracetic acid disinfection protocol on the biocompatibility and biomechanical properties of human patellar tendon allografts. *Cell Tissue Bank* 5:149–160. <https://doi.org/10.1023/B:CATB.0000046071.11459.bd>
- Nicholls SP, Gathercole LJ, Shah JS (1984) Morphology of human palmaris longus tendon. *Ann Rheum Dis* 43:477–482. <https://doi.org/10.1136/ard.43.3.477>
- Olde Damink LH, Dijkstra PJ, van Luyn MJ, van Wachem PB, Nieuwenhuis P, Feijen J (1996a) Cross-linking of dermal sheep collagen using a water-soluble carbodiimide. *Biomaterials* 17:765–773. [https://doi.org/10.1016/0142-9612\(96\)81413-x](https://doi.org/10.1016/0142-9612(96)81413-x)
- Olde Damink LH, Dijkstra PJ, van Luyn MJ, van Wachem PB, Nieuwenhuis P, Feijen J (1996b) In vitro degradation of dermal sheep collagen cross-linked using a water-soluble carbodiimide. *Biomaterials* 17:679–684. [https://doi.org/10.1016/0142-9612\(96\)86737-8](https://doi.org/10.1016/0142-9612(96)86737-8)
- Powell HM, Boyce ST (2006) EDC cross-linking improves skin substitute strength and stability. *Biomaterials* 27:5821–5827. <https://doi.org/10.1016/j.biomaterials.2006.07.030>

- Scheffel DL, Bianchi L, Soares DG, Basso FG, Sabatini C, de Souza Costa CA, Pashley DH, Hebling J (2015) Trans-dentinal cytotoxicity of carbodiimide (EDC) and glutaraldehyde on odontoblast-like cells. *Oper Dent* 40:44–54. <https://doi.org/10.2341/13-338-1>
- Schindelin J, Arganda-Carreras I, Frise E, Kaynig V, Longair M, Pietzsch T, Preibisch S, Rueden C, Saalfeld S, Schmid B et al (2012) Fiji: an open-source platform for biological-image analysis. *Nat Methods* 9:676–682. <https://doi.org/10.1038/nmeth.2019>
- Schmidt EC, Chin M, Aoyama JT, Ganley TJ, Shea KG, Hast MW (2019) Mechanical and Microstructural Properties of Pediatric Anterior Cruciate Ligaments and Autograft Tendons Used for Reconstruction. *Orthop J Sports Med* 7:2325967118821667. <https://doi.org/10.1177/2325967118821667>
- Seto A, Gatt CJ Jr, Dunn MG (2008) Radioprotection of tendon tissue via crosslinking and free radical scavenging. *Clin Orthop Relat Res* 466:1788–1795. <https://doi.org/10.1007/s11999-008-0301-9>
- Shepherd JH, Ghose S, Kew SJ, Moavenian A, Best SM, Cameron RE (2013) Effect of fiber crosslinking on collagen-fiber reinforced collagen-chondroitin-6-sulfate materials for regenerating load-bearing soft tissues. *J Biomed Mater Res A* 101:176–184. <https://doi.org/10.1002/jbm.a.34317>
- Song W, Tang Y, Qiao J, Li H, Rong B, Yang S, Wu Y, Yan X (2019) The short-term safety evaluation of corneal crosslinking agent-genipin. *Ophthalmic Res* 62:141–149. <https://doi.org/10.1159/000499571>
- Suarez LS, Richmond JC (2007) Overview of procurement, processing, and sterilization of soft tissue allografts for sports medicine. *Sports Med Arthrosc Rev* 15:106–113. <https://doi.org/10.1097/JSA.0b013e3180dca1fe>
- Suzuki D, Otsubo H, Watanabe T, Kamiya T, Nagoya S, Yamashita T, Shino K (2015) Ultrastructure of the three anterior cruciate ligament bundles. *Clin Anat* 28:910–916. <https://doi.org/10.1002/ca.22586>
- Takahashi N, Kametani K, Ota R, Tangkawattana P, Iwasaki T, Hasegawa Y, Ueda H, Hosotani M, Watanabe T (2021) Three-dimensional ultrastructure reconstruction of tendinous components at the bifurcation of the bovine superficial digital flexor tendon using array and STEM tomographies. *J Anat* 238:63–72. <https://doi.org/10.1111/joa.13294>
- Ulubayram K, Aksu E, Gurhan SI, Serbetci K, Hasirci N (2002) Cytotoxicity evaluation of gelatin sponges prepared with different cross-linking agents. *J Biomater Sci Polym Ed* 13:1203–1219. <https://doi.org/10.1163/156856202320892966>
- Veríssimo DM, Leitão RF, Ribeiro RA, Figueiró SD, Sombra AS, Góes JC, Brito GA (2010) Polyanionic collagen membranes for guided tissue regeneration: effect of progressive glutaraldehyde cross-linking on biocompatibility and degradation. *Acta Biomater* 6:4011–4018. <https://doi.org/10.1016/j.actbio.2010.04.012>
- Wang Y, Wang X, Shang J, Liu H, Yuan Y, Guo Y, Huang B, Zhou Y (2017) Repairing the ruptured annular fibrosus by using type I collagen combined with citric acid, EDC and NHS: an in vivo study. *Eur Spine J* 26:884–893. <https://doi.org/10.1007/s00586-016-4898-1>
- Wang Z, Liu H, Luo W, Cai T, Li Z, Liu Y, Gao W, Wan Q, Wang X, Wang J et al (2020) Regeneration of skeletal system with genipin crosslinked biomaterials. *J Tissue Eng* 11:2041731420974861. <https://doi.org/10.1177/2041731420974861>
- Xiao D, Zhang Y, Wang R, Fu Y, Zhou T, Diao H, Wang Z, Lin Y, Li Z, Wen L et al (2019) Emodin alleviates cardiac fibrosis by suppressing activation of cardiac fibroblasts via upregulating metastasis associated protein 3. *Acta Pharm Sin B* 9:724–733. <https://doi.org/10.1016/j.apsb.2019.04.003>
- Xu MY, Zhang HR, Zhang L, Zhang H, Yang L, Liu J, Li J, Qiao RQ, Zhang JY, Hu YC (2021) Peracetic acid-ethanol processed human tendon allograft: a morphological, biochemical, and biomechanical study in vitro. *Orthop Surg*. <https://doi.org/10.1111/os.13030>
- Yang X, Feng J, Wang F, Hu Y (2019) Irradiation sterilization used for allogeneic tendon: a literature review of current concept. *Cell Tissue Bank* 20:129–139. <https://doi.org/10.1007/s10561-019-09756-9>
- Yanke AB, Bell R, Lee A, Kang RW, Mather RC 3rd, Shewman EF, Wang VM, Bach BR Jr (2013) The biomechanical effects of 1.0 to 1.2 Mrad of  $\gamma$  irradiation on human bone-patellar tendon-bone allografts. *Am J Sports Med* 41:835–840. <https://doi.org/10.1177/0363546512473816>
- Yeh WL, Lin SS, Yuan LJ, Lee KF, Lee MY, Ueng SW (2007) Effects of hyperbaric oxygen treatment on tendon graft and tendon-bone integration in bone tunnel: biochemical and histological analysis in rabbits. *J Orthop Res* 25:636–645. <https://doi.org/10.1002/jor.20360>
- Zeeman R, Dijkstra PJ, van Wachem PB, van Luyn MJ, Hendriks M, Cahalan PT, Feijen J (1999) Successive epoxy and carbodiimide cross-linking of dermal sheep collagen. *Biomaterials* 20:921–931. [https://doi.org/10.1016/s0142-9612\(98\)00242-7](https://doi.org/10.1016/s0142-9612(98)00242-7)
- Zhou M, Zhang N, Liu X, Li Y, Zhang Y, Wang X, Li B, Li B (2014) Tendon allograft sterilized by peracetic acid/ethanol combined with gamma irradiation. *J Orthop Sci* 19:627–636. <https://doi.org/10.1007/s00776-014-0556-9>

**Publisher's Note** Springer Nature remains neutral with regard to jurisdictional claims in published maps and institutional affiliations.

Springer Nature or its licensor (e.g. a society or other partner) holds exclusive rights to this article under a publishing agreement with the author(s) or other rightsholder(s); author self-archiving of the accepted manuscript version of this article is solely governed by the terms of such publishing agreement and applicable law.